Quasi–*in situ* neutron tomography on polymer electrolyte membrane fuel cell stacks

I. Manke[a)]
Faculty 3, Technical University Berlin, 10623 Berlin, Germany

Ch. Hartnig, M. Grünerbel, J. Kaczerowski, and W. Lehnert
Centre for Solar Energy and Hydrogen Research, 89081 Ulm, Germany

N. Kardjilov, A. Hilger, and J. Banhart
Hahn-Meitner Institute Berlin, 14109 Berlin, Germany

W. Treimer and M. Strobl
University of Applied Sciences, Luxemburger Str. 10, 13353 Berlin, Germany

Quasi–*in situ* neutron tomography is applied to polymer electrolyte membrane fuel cell stacks for a cell-by-cell detection of liquid water agglomerates. Water distributions in the corresponding anodic and cathodic flow fields are analyzed separately. The influence of the membrane thickness as well as effects of the electro-osmotic drag and of back-diffusion from the cathode to the anode on the water distribution are investigated. Furthermore, the well-known engineering problem of the anomalous behavior of the outermost cells in long multistacks is addressed. The suitability of neutron tomography to support the development of fuel cells is shown. © *2007 American Institute of Physics*. [DOI: 10.1063/1.2734171]

In polymer electrolyte membrane (PEM) fuel cells, hydrogen and oxygen react and form water. Thereby, chemical energy is turned into thermal and, due to the separation of the anodic and cathodic processes, electric energies.[1–3] In the anodic reaction hydrogen is oxidized to protons which migrate through the membrane and recombine with oxygen on the surface of the cathodic catalyst, thus forming water. In low temperature PEM fuel cells water plays a crucial role: On the one hand, only the wet membrane is proton conductive. A dry polymer membrane changes its structure and the conductivity of the membrane collapses.[1] On the other hand, flooding is a significant source of power losses during fuel cell operation. Whenever the catalyst layer and the adjacent gas diffusion layers are filled with liquid water, the transport of reactant and product gases (O_2, H_2, and H_2O) is strongly hindered and the supply of the reactive areas is no longer sufficient.

In recent years a growing interest in these issues[4–9] has been observed, but a thorough insight into the fundamental processes of liquid water evolution and transport is still not available. Thus, a specific strategy for component development is missing. Up to now, there are only a few techniques for *in situ* investigations available. Methods using a special cell preparation, e.g., optically transparent components, produce unpredictable disturbances of the system.[10,11]

Neutron radiography has been found to be a valuable tool for *in situ* investigations of water transport in the flow fields and gas diffusion layers.[12–15] The strong interaction of neutrons with hydrogen is exploited to visualize small accumulations of liquid water which are normally shielded by metallic end plates and other components (which can be penetrated by neutrons).

Radiographic methods do not allow for a separate analysis of water on the cathode and anode. Sometimes these drawbacks are solved by using different flow field designs on either side. Otherwise, if the anodic and cathodic flow fields bear a large overlap or are operated in co-flow mode, a distinction of the two contributions cannot be obtained easily. From an application point of view, normally, fuel cell stacks are considered. The water and thermal management and thus the water distribution in the cells differ strongly between single cells and cell stacks, and it is not always possible to derive conclusions from one to the other. Therefore, radiography is of limited use for investigations of fuel cell stacks or single cells with overlapping flow field designs since a separation of the water distribution in each cell or separate electrodes is practically impossible.

The aforementioned problems have been overcome by neutron tomography. This method was applied to fuel cell investigations by Satija *et al.*[14] for structural measurements on a water-free fuel cell. Up to now, the main obstacle in applying tomography to operating fuel cells was the relatively long measuring times of up to several hours for "standard" fuel cells with typical edge sizes between 10 and 20 cm. A tomogram is reconstructed from several hundred single radiographic projections, each requiring typically 10–60 s exposure time. Within the overall measurement time the water distribution normally changes significantly and the tomographic image is rendered useless. Only for very small fuel cells the exposure times can be reduced to a couple of minutes which, however, is still not satisfying.

We carried out quasi–*in situ* neutron tomographies on fuel cell stacks: By switching off the gas flow and temperature regulation the local water distributions in the fuel cell stacks were "frozen" for several hours, thus fulfilling the precondition for realistic imaging by neutron tomography. With this quasi–*in situ* approach we compare water distributions in separate cells within a threefold and a fivefold stack and analyze back-diffusion and the so-called "end-cell problem."

The investigated fuel cells consist of serpentine flow fields with 1 mm wide ribs and channels that were machined
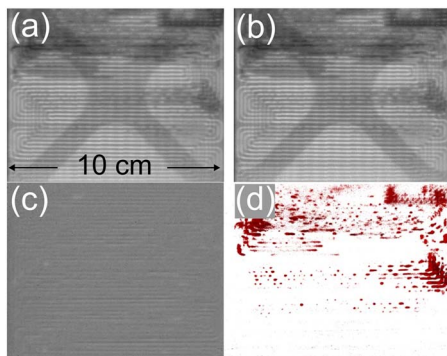
---

a)Electronic mail: manke@hmi.de

FIG. 1. (Color online) Neutron radiogram of a triple fuel cell stack: (a) right before shut off and (b) several hours after a tomography was performed. (c) Quotient of images (a) and (b); (d) neutron tomogram showing the three-dimensional water distribution.
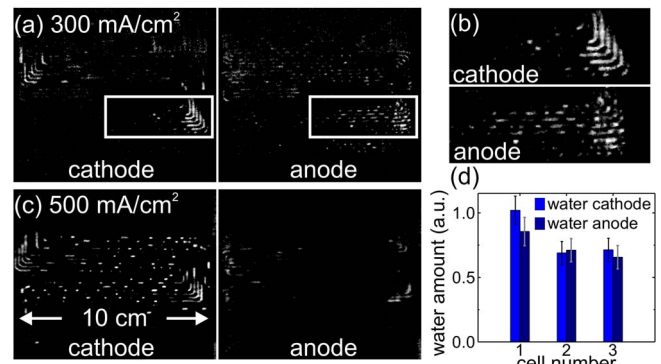

FIG. 2. (Color online) (a) Water distributions in the anodic (left) and cathodic (right) flow field channels of the first cell in a triple fuel cell stack ($i_0 = 300$ mA/cm^2); (b) corresponding enlargements of the marked areas. (c) Water distributions at higher current density ($i_0 = 500$ mA/cm^2). (d) Total water content in the anodic and cathodic flow fields of all three cells at $i_0 = 300$ mA/cm^2.

into separate blank graphite composite plates with 5 and 11 channels on the anode and cathode, respectively. The flow fields have an electrochemically active area of 10×10 cm^2. Cooling flow fields were applied to each side to ensure a proper tempering of the cell; Gore Primea membranes (series 57 with a thickness of 19 μm for the triple stack and series 56 with a thickness of 38 μm for the fivefold stack) and SGL gas diffusion layers (Sigracet 10 BB) were employed for the fuel cell setup. The upright positioned fuel cells were operated at typical parameter settings: $u_C = 25\% - 50\%$, $u_A = 80\% - 90\%$, $T = 55$ °C, and $i_0 = 300$ or 500 mA/cm^2, with u_C and u_A being the utilization ratios of the cathodic and anodic gas streams, T the temperature of the thermostat, and i_0 the current density. The cathodic gas stream was humidified at a dew point of 25 °C, while the anode remained unhumidified. Ambient pressure was kept at the media outlets.

Neutron tomographies were carried out at the CONRAD/V7 facility of the Hahn-Meitner Institute Berlin (BER II research reactor). For each tomography 600 single projections were taken with an exposure time of 30 s per projection. The distance between the rotation axis of the fuel cell stack and the scintillator screen was 9.5 cm. While rotating, the maximal distance of the outermost parts of the active areas (flow field edges) to the screen was 14.5 cm. In a separate measurement the spatial resolution was determined to be about 250 μm at the rotation axis and about 300 μm at the outermost position (for $L/d = 500$). The neutron flux was nonuniformly distributed over the active area of the fuel cell stack with values between $(3$ and $6) \times 10^6$ neutrons/cm^2 s.

In Fig. 1(a) a radiographic projection of a triple stack is given. The stack was operated at $u_A = 80\%$, $u_C = 40\%$ (humidified cathode), and $i_0 = 330$ mA/cm^2. The active area can be identified by the horizontal lines of the flow field channels. In the upper part, some of the flow field channels are filled with water, which causes the observed dark shadows. After acquiring this image the gas flow and the temperature regulation were shut off and the gas interconnections were sealed to keep the water distribution in the channels constant for several hours. Only minor changes are caused by this procedure, especially at the vertical turns of the flow field channels where water droplets are affected by gravity. About three hours later a tomographic measurement was started, which took 5 h. A three-dimensional view of the resulting tomogram is displayed in Fig. 1(d). Only the water distribution in the channels is shown, whereas all cell components

have been made transparent. The viewing direction is the same as in the radiograph of Fig. 1(a). In Fig. 1(b) a radiographic projection taken after the tomographic run is displayed. It can be compared to Fig. 1(a) and serves as a validation of the assumption of a stationary water distribution. The quotient of images (a) and (b) [Fig. 1(c)] shows the changes in the local neutron transmission between both images. Some small changes are mainly caused by a slight movement of the fuel cell during measurement.

The tomogram shown in Fig. 1(d) was used to analyze the water distribution in different cells and the corresponding cathodes and anodes of the triple stack. In Fig. 2(a) the water distributions in the cathodic (left) and the anodic (right) flow fields of the first cell in the stack are displayed. Again, only water (white) is shown, while the other components have been made transparent. Due to different flow conditions at the turns of the flow field channels,[16] most water has accumulated in these areas of the flow field [Fig. 2(b)].

Despite the external humidification of the cathodic gas stream and the fact that the cathode is the "water producing" electrode, the amounts of water in the cathodic and anodic flow field channels are almost identical. This can be explained by back-diffusion from the cathode to the anode which is one of the key factors for a uniform humidification of the active area of the fuel cell.

For cathode and anode in each cell the amount of water was calculated by summing over the various water containing volume parts. Only water clusters larger than the spatial resolution (≥ 300 μm) are taken into account by this method. However, as the flow field surface is hydrophobic, preferably larger water clusters are formed, and therefore the majority of liquid water in the flow field channels is detected. Figure 2(d) shows the calculated amount of water in the cathodic and anodic channels of each cell at $i_0 = 300$ mA/cm^2. The different cell parts contain a comparable amount of water, with rather small variations around 20%–30%. The estimated measurement errors of around 10% are based on the choice of threshold and beam hardening artifacts.

The balance between the two reverse effects, back-diffusion and electro-osmotic drag (i.e., reduced water back-diffusion due to the proton flux from anode to cathode), is shifted at higher current densities (i.e., higher proton fluxes). In order to analyze this effect a tomogram was taken at $i_0 = 500$ mA/cm^2. Corresponding water distributions are dis-
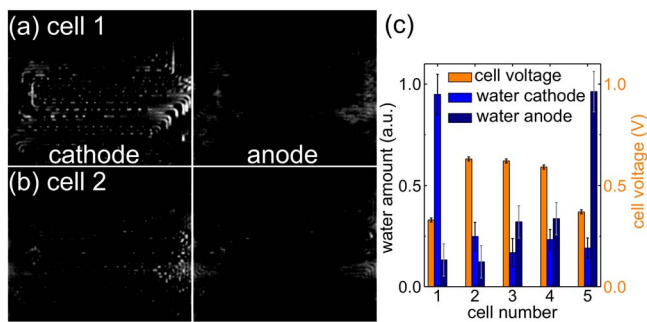
FIG. 3. (Color online) Water distribution in a fivefold fuel cell stack along the cathodes (left) and anodes (right) of the outermost (a) and the second cell (b). (c) Total water content in the ten anodic and cathodic flow fields and the corresponding averaged cell voltages at $i_0 = 500$ mA/cm^2.

played in Fig. 2(c). The amount of water on the anode is strongly reduced. Almost no liquid water can be detected in the anodic flow field channels.

The results of the triple stack are compared to a tomographic investigation of a fivefold stack with a thinner membrane (57 series instead of 56 series, see above) at the same operating conditions. From this stack size onwards the so-called end-cell problem is often observed: the two outermost cells show a decreased performance compared to the inner cells. Figures 3(a) and 3(b) show the water distributions in the cathodic (left) and anodic (right) flow field channels of the first two cells in the stack [(a) and (b)]. The pattern of the water clusters is similar to the one observed in the shorter triple stack (agglomerates in the turns of the flow field). Contrary to the results for a short stack, the amount of water in the cathodic flow field of the first cell is much larger than for the other cell parts. An overview of the water distribution between anodes and cathodes of each of the five cells is given in Fig. 3(c). The results reveal not only a significant larger amount of water on the cathode side of the first cell (as shown before), but also a comparable water amount in the anodic flow field of the last cell. Correlated to this increased water content, the average cell voltage (i.e., the electric performance) is decreased in these two cells.

In the inner cells the amounts of liquid water are lower and, at the same time, the performances are up to 50% higher. Here, the liquid water contents vary only slightly between the different cells. Despite the rather high current density of $i_0 = 500$ mA/cm^2, the variations between the respective anodic and cathodic sides are rather small.

From the latter result it can be concluded that the thinner membrane used in this cell setup (compared to the setup for the triple stack) leads to an equilibration of the electro-osmotic drag by back-diffusion and thus to a well-balanced water distribution even at increased current densities.

The increased water content in the outermost cells can be related to slight thermal deviations: the cathode of cell 1 and the anode of cell 5 are in direct contact with the corresponding end plates. Even though the temperature of the stack is controlled, the influence of a minor, unavoidable temperature drop could lead to a strongly increased formation of liquid water as can be deduced from the water vapor saturation curve. The resulting water agglomerates then lead

to an overall reduction of the effective cross section of the flow field channel and, at the same time, to a decreased reactant gas flow in these cells, causing amongst other factors a reduced power output. Adapted designs of the outermost flow fields or improved insulation might be considered to circumvent these effects and to enhance the performance of the end cells.

In conclusion, quasi–*in situ* neutron tomography has been proven to be an excellent method to analyze the water distribution in operating fuel cell stacks three dimensionally. A separate analysis of water accumulations in the different cells in the stack and, furthermore, a separation into anodic and cathodic contributions are possible and allow for a thorough insight into the effects of material properties on water management. The back-diffusion of liquid water from cathode to anode is significantly reduced at increased current densities due to the increased electro-osmotic drag when thicker membranes are used; a more equilibrated distribution has been observed when thinner membranes are employed. Thermal effects might lead to an enhanced condensation of liquid water and cause deviations in the gas flow and pressure of the outermost cells in longer stacks, resulting in a decreased performance of these cells. These effects are not as pronounced in triple stacks compared to fivefold ones but might play an even more important role in longer stacks. In the future neutron tomography could greatly enhance the possibilities of neutron imaging for *in situ* investigations of fuel cells and could help to solve current problems in fuel cell development.

[1] *Handbook of Fuel Cells: Fundamentals, Technology and Applications* (Wiley, Chichester, 2003), Vol. 3, pp. 337-347.

[2] B. C. H. Steele and A. Heinzel, Nature (London) **414**, 345 (2001).

[3] L. Carrette, K. A. Friedrich, and U. Stimming, Fuel Cells **1**, 5 (2001).

[4] U. Pasaogullari and C. Y. Wang, J. Electrochem. Soc. **152**, 380 (2005).

[5] A. A. Kulikovsky, T. Wüster, A. Egmen, and D. Stolten, J. Electrochem. Soc. **152**, A1290 (2005).

[6] G. Lin, W. He, and T. Van Nguyen, J. Electrochem. Soc. **151**, 1999 (2004).

[7] C. Ziegler, H. M. Yu, and J. O. Schumacher, J. Electrochem. Soc. **152**, 1555 (2005).

[8] P. Berg, K. Promislow, J. St. Pierre, J. Stumper, and B. Wetton, J. Electrochem. Soc. **151**, 341 (2004).

[9] S. Litster, D. Sinton, and N. Djilali, J. Power Sources **154**, 95 (2006).

[10] X. G. Yang, F. Y. Zhang, A. L. Lubawy, and C. Y. Wang, Electrochem. Solid-State Lett. **7**, 408 (2004).

[11] K. Tüber, D. Pócza, and C. Hebling, J. Power Sources **124**, 403 (2003).

[12] M. M. Mench, Q. L. Dong, and C. Y. Wang, J. Power Sources **124**, 90 (2003).

[13] R. J. Bellows, M. Y. Lin, M. Arif, A. K. Thompson, and D. Jacobson, J. Electrochem. Soc. **146**, 1099 (1999).

[14] R. Satija, D. L. Jacobson, M. Arif, and S. A. Werner, J. Power Sources **129**, 238 (2004).

[15] J. Zhang, D. Kramer, R. Shimoi, Y. Ono, E. Lehmann, A. Wokaun, K. Shinohara, and G. G. Scherer, Electrochim. Acta **51**, 2715 (2006).

[16] N. Pekula, K. Heller, P. A. Chuang, A. Turhan, M. M. Mench, J. S. Brenizer, and K. Ünlü, Nucl. Instrum. Methods Phys. Res. A **542**, 134 (2005).